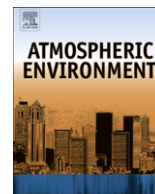




Contents lists available at SciVerse ScienceDirect

## Atmospheric Environment

journal homepage: [www.elsevier.com/locate/atmosenv](http://www.elsevier.com/locate/atmosenv)

## Measurements of formaldehyde at the U.S.–Mexico border during the Cal-Mex 2010 air quality study

Jun Zheng<sup>a,b</sup>, Renyi Zhang<sup>b,\*</sup>, Jessica P. Garzón<sup>b,c</sup>, María E. Huertas<sup>b,c</sup>, Misti Levy<sup>b</sup>, Yan Ma<sup>a</sup>, Ricardo Torres-Jardón<sup>d</sup>, Luis G. Ruiz-Suárez<sup>d</sup>, Lynn Russell<sup>e</sup>, Satoshi Takahama<sup>e</sup>, Haobo Tan<sup>f</sup>, Guohui Li<sup>g</sup>, L.T. Molina<sup>g</sup>

<sup>a</sup>Jiangsu Key Laboratory of Atmospheric Environment Monitoring and Pollution Control, Nanjing University of Information Science & Technology, Nanjing 210044, China

<sup>b</sup>Department of Atmospheric Sciences, Texas A&M University, College Station, TX 77843-3150, United States

<sup>c</sup>Tecnológico de Monterrey, Eduardo Monroy Cardenas No. 2000, Toluca, Mexico

<sup>d</sup>Centro de Ciencias de la Atmósfera, Universidad Nacional Autónoma de México, Mexico

<sup>e</sup>Scripta Institution of Oceanography, University of California San Diego, La Jolla, CA 92093, United States

<sup>f</sup>Institute of Tropical and Marine Meteorology, CMA, Guangdong 510080, China

<sup>g</sup>Molina Center for Energy and The Environment, La Jolla, CA 92037, United States

## H I G H L I G H T S

- We measured HCHO using a fast-response PTR-MS during the Cal-Mex 2010 study.
- Up to 13.7 ppbv HCHO was measured along the Tijuana–San Diego boarder.
- In this study, HCHO was found to be more important than O<sub>3</sub> in contributing to OH radicals and the local photochemistry.

## A R T I C L E I N F O

## Article history:

Received 2 August 2012

Received in revised form

15 September 2012

Accepted 17 September 2012

## Keywords:

Formaldehyde

PTR-MS

Ozone

Hydroxyl radical

Secondary organic aerosol

Air pollution

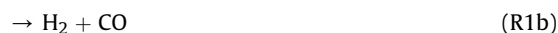
## A B S T R A C T

Ambient formaldehyde (HCHO), along with other volatile organic compounds (VOCs), was measured using proton-transfer reaction mass spectrometry (PTR-MS) at a ground site along the U.S.–Mexico border during the Cal-Mex 2010 air quality study. During the observation period, the HCHO mixing ratio varied between 1.0 ppbv and 13.7 ppbv. On average, a daily maximum of  $6.3 \pm 2.6$  ppbv occurred around 10 AM and a minimum of  $2.8 \pm 1.3$  ppbv was observed around midnight. The early onset of the HCHO daily maximum ( $\sim 3$  h before the solar noon) indicated the presence of primary HCHO sources and a fast photolysis loss of HCHO, consistent with a measured low ratio of HCHO to acetaldehyde of ( $2.5 \pm 0.8$ ). Using the simulated photolysis rates, we estimated the contribution of OH radical production from HCHO photolysis relative to that from O<sub>3</sub> photolysis, with a ratio from 0.8 to 18 and the highest values around traffic rush hours. Hence, our results indicate that HCHO plays a dominant role in regulating the OH radical budget in the area.

© 2012 Elsevier Ltd. All rights reserved.

## 1. Introduction

HCHO is of importance in atmospheric chemistry as one of the most abundant carbonyl compounds and a major precursor of free radicals in the atmosphere (Dasgupta et al., 2005). Since the absorption spectrum of HCHO extends to a longer wavelength range than other aldehydes, HCHO has a much higher photolysis frequency and hence contributes considerably to free radical productions at the ground level (Finlayson-Pitts and Pitts, 1999),



Two radicals are formed through channel (R1a) and are subsequently converted into hydroperoxyl radicals (HO<sub>2</sub>) in the presence of O<sub>2</sub> (R2 and R3), which are actively involved in the photochemical cycles, responsible for ground-level ozone formation and degradations of most primary air pollutants (Finlayson-Pitts and Pitts,

\* Corresponding author.

E-mail addresses: [Renyi-Zhang@geos.tamu.edu](mailto:Renyi-Zhang@geos.tamu.edu), [renyi-zhang@tamu.edu](mailto:renyi-zhang@tamu.edu) (R. Zhang).

1999; Zhang et al., 2003). HCHO has a relatively short lifetime ( $\sim$ a few hours) (Finlayson-Pitts and Pitts, 1999) due to photolysis (R1) and reaction with hydroxyl radical (OH),



It is worth noting that reaction (R4) does not affect  $\text{HO}_x$  ( $\text{OH} + \text{HO}_2$ ) radical budget because of reaction (R3).

HCHO can be formed from the photochemical oxidation of many volatile organic compounds (VOCs) (Fan and Zhang, 2004; Finlayson-Pitts and Pitts, 1999), among which isoprene has the highest HCHO formation potential (Okuyama et al., 1984; Zhang et al., 2002). During the biogenic growing season, HCHO formation is virtually dominated by isoprene emission (Wagner and Wyszynski, 1996). Although the  $\text{CH}_4$  reaction with OH is relatively slow (at 298 K,  $k_{\text{CH}_4+\text{OH}} < 1 \times 10^{-14} \text{ cm}^3 \text{ molecules}^{-1} \text{ s}^{-1}$ ) (Atkinson and Arey, 2003), the high  $\text{CH}_4$  mixing ratio ( $\sim 2 \text{ ppmv}$ ) (Finlayson-Pitts and Pitts, 1999) constitutes the primary precursor of HCHO in the background atmosphere. HCHO is also emitted directly into the air by both natural and anthropogenic processes. Biomass burning and animal excretion represent the most important natural primary HCHO sources (Carlier et al., 1986). However, anthropogenic sources are more important in terms of magnitude and diversity, such as petrochemical production, chemical synthesis of plastics and paints, and incomplete combustions of fossil fuels (Carlier et al., 1986). For example, a high concentration of HCHO has been observed around the Houston Ship Channel refinery compounds (Friedfeld et al., 2002; Rappengluck et al., 2010; Buzcu Guven and Olaguer, 2011), and automobile exhausts are identified as the most common primary emission source in the populated urban areas (Anderson et al., 1996), yielding HCHO as one of the most abundant components of internal-combustion engine exhausts (Wagner and Wyszynski, 1996). Diesel vehicles emit higher levels of formaldehyde than do gasoline vehicles.

In recent years, the usage of alternative and reformulated fuels (such as natural gas and methanol/ethanol blended gasoline, or methyl-*t*-butyl ether as an additive for gasoline) has been greatly promoted for the purpose of reducing smog-forming and toxic pollutants emission. However, such fuels may substantially increase HCHO emission (Alzueta and Glarborg, 2003; Bravo and Torres, 2000; Mitchell and Olsen, 2000). Using a statistical method with carbon monoxide (CO) and ozone ( $\text{O}_3$ ) as the tracers of primary and secondary HCHO respectively, Friedfeld et al. (2002) found that about 37% of HCHO observed in Houston were attributed to primary emission. However, a recent study by Parrish et al. (2012) using emission inventory constrained by field measurements concluded that the primary sources only contribute to about 5% of the total HCHO in the Houston area. An understanding of the atmospheric abundance of HCHO is essential in assessing the OH radical budget, the degradation of other primary air pollutants, and formation of secondary pollutants, including ozone and secondary organic aerosols (Fan et al., 2006; Zhao et al., 2006, 2009; Zhang et al., 2009).

Several HCHO measurement techniques have been developed, and a comprehensive review of the HCHO detection methods have been provided by J.Z. Li et al. (2005). In particular, the method of proton-transfer reaction mass spectrometry (PTR-MS) has been employed for fast measurements of HCHO (Karl et al., 2003), although the proton affinity of HCHO is only slightly higher than that of water. HCHO is routinely monitored during air quality studies as an important indicator of the photochemical reactivity. In the U.S. urban areas, HCHO concentration varies from a few ppbv to about 20 ppbv (Dasgupta et al., 2005; Lee et al., 1998). A comparable or higher level of HCHO has been observed in the Mexico City Metropolitan Area (Lei et al., 2009; Volkamer et al., 2010), because partially of direct emissions from automobiles.

We report the HCHO measurements using PTR-MS during the Cal-Mex 2010 field campaign. The humidity dependency of the PTR-MS is evaluated and the dataset is validated. An advantage using the PTR-MS approach is that, along with HCHO, a suite of oxygenated VOCs are simultaneously measured by the PTR-MS. The objective of this research is to evaluate the contribution of HCHO to the daytime OH budget in the San Diego-Tijuana area, which is fundamentally responsible for the chemical evolutions of both gaseous and particulate pollutants.

## 2. Experimental methods

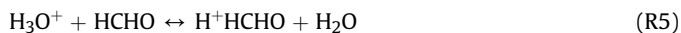
### 2.1. Measurement overview

From 15 May to 30 June 2010, HCHO and VOC measurements were conducted as part of the Cal-Mex 2010 air quality study, designed to identify primary emission sources and to investigate the atmospheric processes, controlling the air pollutants formation and transport along the Mexico-California border region. The observation site of the current work is near the urban center of Tijuana, Baja California, Mexico, inside the Parque Morelos ( $32^\circ 29' 49.33''\text{N}$ ,  $116^\circ 56' 31.21''\text{W}$ ) (Fig. 1). A more detailed description of the site has been given in a companion paper (Zheng et al., submitted for publication) of this special issue. The data in this work are recorded in local time, i.e., Pacific Daylight Time (PDT).

### 2.2. PTR-MS

A commercial PTR-MS (Ionicon Analytik) was used in this work to measure HCHO, acetaldehyde ( $\text{CH}_3\text{CHO}$ ) and other VOCs. The PTR-MS consisted of an ion source, a drift tube reactor and a quadrupole mass spectrometer (QMS). In principle, any VOC with a proton affinity (PA) higher than water ( $166.5 \text{ kcal mol}^{-1}$ ) can be ionized through proton transfer reaction with hydronium ion ( $\text{H}_3\text{O}^+$ ) and detected by the QMS (Hansel et al., 1995; Lindinger et al., 1998; Zhao and Zhang, 2004). A detailed description of the PTR-MS operation principles of the current work has been provided elsewhere (Zhao and Zhang, 2004; Zhao et al., 2004, 2005a; Zheng et al., submitted for publication), and only information pertinent to the HCHO measurement is discussed below. Briefly, the drift tube was operated at 1.98 mbar,  $50^\circ\text{C}$  and the electric field was maintained at  $50 \text{ V cm}^{-1}$ , equivalent to an  $\text{E/N}$  ratio of 113 Townsend ( $1\text{Td} = 10^{-17} \text{ V cm}^2$ ). The typical ion-molecular reaction time was about  $1.3 \times 10^{-4} \text{ s}$ . Water vapor flow in the ion source was maintained at 8 sccm.

HCHO was detected at  $m/z = 31$ . Since HCHO has a PA ( $170.4 \text{ kcal mol}^{-1}$ ) only slightly higher than water, protonated HCHO ( $\text{H}^+\text{HCHO}$ ) can undergo proton transfer reaction with neutral water, i.e., (R5) is reversible.



The kinetics expression for protonated formaldehyde is

$$\frac{d[\text{H}^+\text{HCHO}]}{dt} = k_1[\text{HCHO}][\text{H}_3\text{O}^+] - k'_1[\text{H}^+\text{HCHO}][\text{H}_2\text{O}] \quad (\text{E1})$$

where  $k_1$  and  $k'_1$  are the forward and reverse reaction rate coefficients of (R5), respectively, and  $t$  is the reaction time in the drift tube. Since the sum of  $[\text{HCHO}]$  and  $[\text{H}^+\text{HCHO}]$  is a constant, i.e., the initial HCHO concentration, Eq. (E1) can be solved as

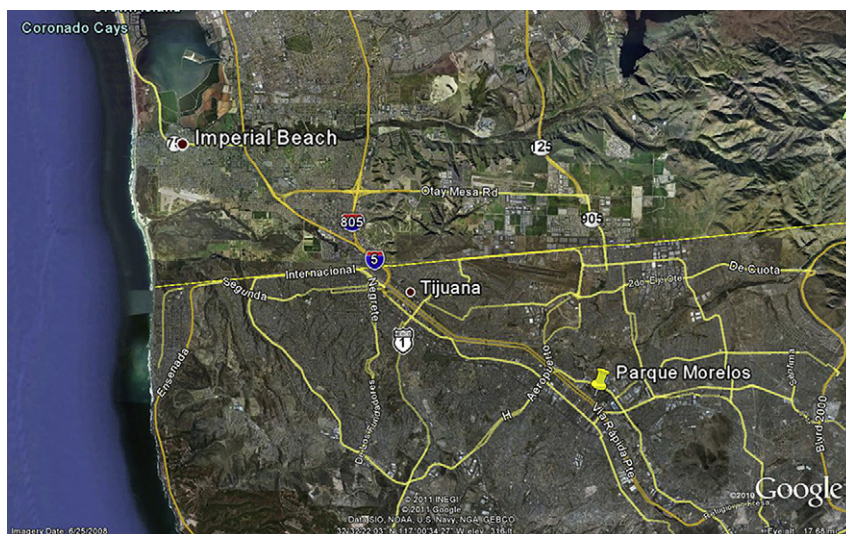


**Fig. 1.** Map of the observation site, Parque Morelos (indicated by the yellow marker), which is about 3.5 mi to the south of the Mexico-U.S. border and ~110 mi to the NE of the highway 5. (For interpretation of the references to colour in this figure legend, the reader is referred to the web version of this article.)

$$[H^+HCHO] = \frac{k_1 [HCHO] [H_3^+O] (1 - e^{-(k_1 [H_3^+O] + k'_1 [H_2O])t})}{k_1 [H_3^+O] + k'_1 [H_2O]} \quad (E2)$$

Since typical  $[H_2O] \gg [H_3^+O]$  (Steinbacher et al., 2004), Eq. (E2) can be simplified as

$$[H^+HCHO] = \frac{k_1 [HCHO] [H_3^+O] (1 - e^{-k'_1 [H_2O]t})}{k'_1 [H_2O]} \quad (E3)$$

Clearly, the sensitivity of PTR-MS for HCHO is a function of the water concentration inside the drift tube, which can originate from both the ion source and the sample flow. To reduce the signal variation due to changes in  $H_3^+O$  intensity,  $H^+HCHO$  and other masses were normalized by  $H_3^+O$  signal. Hence, the sensitivity dependence to water in HCHO detection can be expressed as

$$\frac{[H^+HCHO]}{[H^+HCHO]_{dry}} = \frac{[H_2O]_{dry} (1 - e^{-k'_1 [H_2O]t})}{[H_2O] (1 - e^{-k'_1 [H_2O]_{dry}t})} \quad (E4)$$

where the subscript “dry” denotes the condition when the sample flow was water free.

The primary hydronium ion reacts with water inside the drift tube to form water cluster ( $H_3^+O \cdot H_2O$ ,  $m/e$  37). Due to collisions induced by the electric field in the drift tube,  $H_3^+O \cdot H_2O$  can also be dissociated back into  $H_3^+O$ .



Therefore, the intensity of  $H_3^+O \cdot H_2O$  signal depends on the E/N ratio and water concentration in the drift tube. Since the E/N ratio and water vapor flow in the ion source were kept constant during measurements, the variation of water concentration in the drift tube was solely determined by the sample flow humidity and thus a quantitative correlation could be established between  $m/e = 37$  signal and the ambient water concentration (Ammann et al., 2006). Fig. 2 shows a plot of  $m/e = 37$  against the ambient water mixing ratio ( $\text{mmol mol}^{-1}$ ) during the observation period. The line in Fig. 2 corresponds to a second order polynomial fit of the data as a function of ambient water mixing ratio in the form of  $y = 123x^2 +$

$1390x + 17,900$ , where  $R^2 = 0.88$ . By linearly extrapolating to the condition when no  $m/e = 37$  can be detected using data near the zero ambient humidity, we obtained the water vapor concentration originating from the ion source with a value equivalent to  $12.0 \text{ mmol mol}^{-1}$  or  $5.36 \times 10^{14} \text{ molecules cm}^{-3}$  in the drift tube.

To calibrate the PTR-MS for HCHO measurements, gaseous HCHO standards were generated from diluted HCHO solution (~10% by weight), by dissolving 1,3,5-trioxane powder (Sigma–Aldrich, >99.0%) into pure water ( $R > 16 \text{ M}\Omega$ ). During calibration, a flow of a few sccm dry nitrogen was bubbled through the HCHO solution and fed into an UV/VIS spectrophotometer (Perkin Elmer, Model 552), where the absolute concentration of HCHO vapor was measured by its absorption at 304 nm ( $\sigma = 5.54 (\pm 0.16) \times 10^{-20} \text{ cm}^2 \text{ molecule}^{-1}$ , (Gratien et al., 2007)). Immediate after exiting the absorption cell, the primary HCHO standard (~1000 ppmv) was mixed into ~10 slpm zero air generated from a commercial zero air supply (Thermo Scientific, Model 1160). By varying the primary HCHO vapor flow rate from ~0.5 to 5 sccm, the standard mixing ratio ranged from several tens of ppbv to a few ppmv.

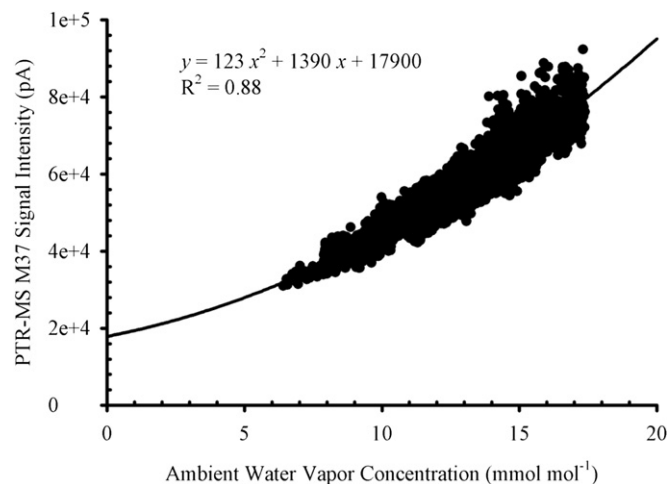


**Fig. 2.** A second order polynomial fit between ambient water vapor concentration and the corresponding M37 signal (pA) detected by the PTR-MS.



The HCHO calibration method described above was based on the well-developed spectrophotometric technique of high precision and reliability. However, the spectrophotometer required relatively well-controlled laboratory operation conditions, which was not available in the field. Therefore, a more portable HCHO permeation device was utilized during the field measurements. The permeation device was similar as the one previously utilized by us for gaseous nitric acid calibrations (Zheng et al., 2008, 2010). Briefly, the device was a temperature-controlled U-shaped glass tube of two symmetric compartments, with one part to hold a HCHO permeation tube (VICI Metronics) and the other part filled with glass beads. When in operation, a flow of about 100 sccm nitrogen was firstly supplied into the side of U-tube filled with glass beads and was warmed to the same temperature as the permeation tube. The nitrogen flow carrying the permeated HCHO vapor was then injected into a stream of zero air of up to a few slpm, resulting in a final HCHO concentration of a few to tens of ppbv. The permeation rate of the HCHO permeation tube was determined by calibration with the HCHO standards quantified by the spectrophotometric method and a value of  $20.5 \pm 2.6 \text{ ng min}^{-1}$  was obtained. Fig. 3 shows a plot of two successive HCHO calibrations with the HCHO standards generated from the HCHO solution and the permeation tube. The PTR-MS response was on the basis of kinetics calculations with an ion-molecular rate coefficient of  $1.4 \times 10^9 \text{ molecule cm}^3 \text{ s}^{-1}$  (Hansel et al., 1997). Evidently, the PTR-MS shows a wide linear dynamic range in the HCHO calibration. The water content in the zero air was considerably lower and the corresponding  $m/e = 37$  signal was about  $2.0 \times 10^4 \text{ pA}$ . Therefore, the PTR-MS sensitivity to HCHO at ambient humidity can be determined according to Eq. (E4), in which the reverse reaction rate coefficient ( $k'_1$ ) was taken as  $3 \times 10^{-11} \text{ cm}^3 \text{ molecule}^{-1} \text{ s}^{-1}$  (Hansel et al., 1997), the reaction time under the present working condition was about  $1.3 \times 10^{-4} \text{ s}$ , and the water concentration was the sum of water originated from the ion source and the ambient sample flow.

$\text{O}_3$  and meteorological parameters were measured using commercial instruments onboard the CCA-UNAM air quality mobile monitoring station. The detailed operation principle and procedures has been provided in a companion paper in this special issue (Zheng et al., submitted for publication). The photolysis rates ( $J$ -values) were calculated using a Fast Tropospheric Ultraviolet–Visible (FTUV) model, which was a modified version of the TUV

model. The detailed setup of the model has been given elsewhere (G.H. Li et al., 2005; Tie et al., 2003, 2005). In this work, the zero cloud coverage condition was assumed and surface albedo was taken as 0.1. Also, it is likely that aerosols exert an impact on light transfer (Zhang et al., 2008; Khalizov et al., 2009), but the influence of aerosols on photolysis has not been accounted for in the present FTUV model. In general, the difference in calculated photolysis rates between the FTUV and the TUV is within 5% in the troposphere.

Organic aerosol (OA) concentration was measured with an Aerodyne Aerosol Chemical Speciation Monitor (ACSM) with a Pfeiffer Prisma quadrupole. The ACSM was a simplified version of the Aerodyne Aerosol Mass Spectrometer with the primary difference being the absence of a particle time-of-flight measurement (Takahama et al., 2012). The measured oxidized OA concentration by ACSM provides an indirect indication of the atmospheric oxidation capability (Aiken et al., 2009, 2010).

### 3. Results and discussions

#### 3.1. HCHO measurements

Fig. 4 displays the HCHO measurements during the observation period. Generally, HCHO mixing ratio varies between 1.0 ppbv and 13.7 ppbv. On average, a daily maximum of  $6.3 \pm 2.6$  ppbv is reached around 10 AM and a minimum of  $2.8 \pm 1.3$  occurs around midnight. The frequency distribution of HCHO (Fig. 4c) is plotted from 4116 sample points. Two thirds of the HCHO data points fall in the range between 1.5 ppbv and 4.0 ppbv and 11 days of the entire period have a daily maximum HCHO exceeding 10 ppbv, comparable with a typical HCHO level observed in the U.S. urban areas (Dasgupta et al., 2005). However, the early onset of daily maximum ( $\sim 3 \text{ h}$  before solar noon) indicates the presence of primary HCHO sources and a fast photolysis loss of HCHO.

The photochemical oxidation processes of biogenic VOCs (e.g., isoprene) tend to yield more HCHO than  $\text{CH}_3\text{CHO}$  (Blanchard, 1999; Okuyama et al., 1984) and hence increase the  $\text{HCHO}/\text{CH}_3\text{CHO}$  ( $C_1/C_2$ ) ratio to a value of 10, which has been observed at a deciduous forested area (Shepson et al., 1991). However, in the urban area both HCHO and  $\text{CH}_3\text{CHO}$  may be emitted from automobiles, leading to a decrease in the  $C_1/C_2$  ratio to  $\sim 1$  (Anderson et al., 1996; Werner et al., 1999). Nevertheless, natural reactive hydrocarbons may be also present in an urban environment to some extent, depending on the availability of vegetation. Therefore, a typical  $C_1/C_2$  ratio observed in an urban area varies between 0.7 and 3.0 (Shepson et al., 1991). In this work, we obtained an average value of  $2.5 \pm 0.8$ , which was comparable with the  $C_1/C_2$  ratio of 0.6–3.1 observed in southern California (Shepson et al., 1991). The relatively low value of  $C_1/C_2$  ratio along the Cal-Mex border is consistent with the facts that the Tijuana region is relatively arid and is mostly covered by xeric scrubs, contributing little to biogenic VOC emissions. In addition, the gasoline supplied in San Diego and Tijuana contains 10% of ethanol, leading to a higher acetaldehyde emission from automobiles (Tanner et al., 1988; Anderson et al., 1996; Anderson, 2009). This finding also implies that aldehydes in Tijuana are highly affected by primary anthropogenic emissions.

#### 3.2. Contribution to the OH radical production

The photolysis of  $\text{O}_3$  and the subsequent reaction with water (R7–R9) are considered the most important OH radical source (Finlayson-Pitts and Pitts, 1999) in terms of the global atmosphere.

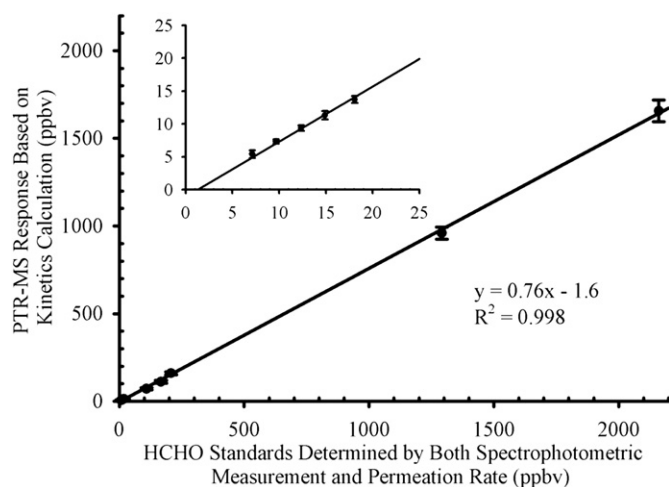
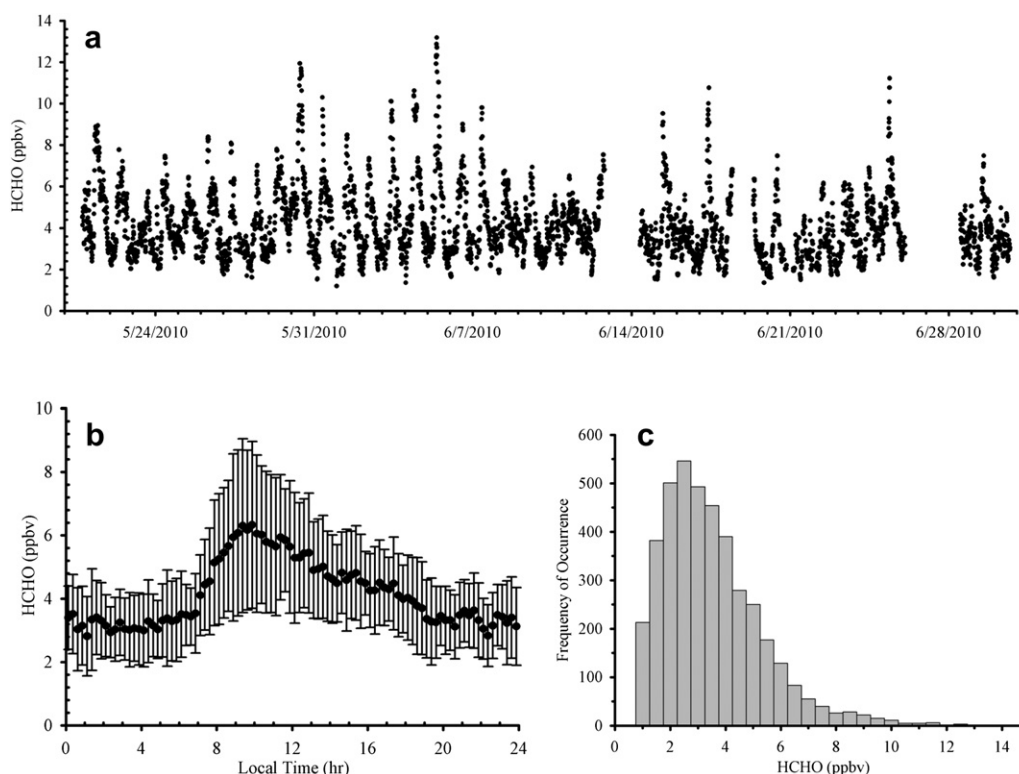


Fig. 3. Linear regression of PTR-MS responses from two successive calibrations with HCHO standards generated from both a HCHO solution and a permeation device. The insert is a blow up of HCHO standards from the permeation tube.



**Fig. 4.** a) Time series of HCHO measured at Parque Morelos, Tijuana, during the Cal-Mex 2010 field studies; b) The diurnal variation of 8-min average HCHO data (black dots) with  $\pm 1$  standard deviation error bar; c) The frequency histogram of the HCHO data.



The formation rate of OH from (R7–R9), denoted as  $P_{\text{OH},\text{O}_3}$ , can be expressed as

$$P_{\text{OH},\text{O}_3} = J_{\text{O}_3}[\text{O}_3] \frac{2k_g[\text{H}_2\text{O}]}{k_g[\text{M}] + k_g[\text{H}_2\text{O}]} \quad (\text{E5})$$

where  $J_{\text{O}_3}$ ,  $k_g$  and  $k_9$  are the photolysis rate of  $\text{O}_3$ , rate coefficients of (R8) and (R9), respectively. The corresponding OH production rate from HCHO photolysis ( $P_{\text{OH},\text{HCHO}}$ ) is determined as

$$P_{\text{OH},\text{HCHO}} = 2J_{\text{HCHO}}[\text{HCHO}] \quad (\text{E6})$$

where  $J_{\text{HCHO}}$  is the photolysis rate of channel (R1a) and all  $\text{HO}_2$  produced from (R1a) is assumed to be completely converted into OH, which is the case during most of the daytime. Therefore, the estimation of  $P_{\text{OH},\text{HCHO}}$  using (E6) is an upper limit.

Fig. 5a depicts the calculated daytime (8 AM–6 PM) OH formation rates because of the photolysis of HCHO and  $\text{O}_3$  and the ratio between the two photolysis rates. For comparison, the corresponding HCHO,  $\text{O}_3$ , and organic aerosol concentrations are also shown in Fig. 5b. It is apparent from Fig. 5a that HCHO is a much stronger OH source than  $\text{O}_3$  during the observation period and the  $P_{\text{OH},\text{HCHO}}/P_{\text{OH},\text{O}_3}$  ratio varies from 0.8 to 18. A prominent feature of Fig. 5a is that  $P_{\text{OH},\text{HCHO}}$  nearly reaches its daily maximum at about 9:30 AM and fluctuates slightly at the similar level until about 12:00 PM. However,  $P_{\text{OH},\text{O}_3}$  exhibits a similar profile as the solar radiation intensity and reaches maximum level around 12:15 PM. A possible explanation is that in the early morning HCHO is most likely originated from primary automobile emissions and reaches its daily maximum several hours earlier than  $\text{O}_3$ . After sunrise, photochemistry begins to contribute to both HCHO and  $\text{O}_3$  productions, despite of dilution due to vertical mixing within the

planetary boundary layer. However, the photolysis of HCHO also causes HCHO to decrease, while maintaining a similar level of OH production until early afternoon. It is interesting to note that the diurnal profile of the oxidized OA concentration measured by ACSM (Fig. 5b) also shows a similar pattern as that of HCHO, i.e., decreasing throughout the afternoon hours (Takahama et al., 2012). In general, oxidation of volatile organic compounds initiated by OH radicals produces various products (Lei et al., 2000a, 2000b; Lei and Zhang, 2001; Zhang et al., 2000), some of which may participate in SOA formation through nucleation and growth processes, i.e., by condensation, partitioning, and heterogeneous reactions (Zhao et al., 2005b; Wang et al., 2010a; Zhang et al., 2012). Our results imply that the SOA production in this region is likely linked to the OH source arising from formaldehyde photolysis (Hodzic and Jimenez, 2011).

It should be pointed out that the  $\text{O}_3$  concentration at Tijuana during the observation period was considerably lower than many North America urban areas, such as Los Angeles (Sakugawa and Kaplan, 1993), Houston (Lei et al., 2004; G.H. Li et al., 2005; Li et al., 2007; Zhang et al., 2004) and Mexico City (Molina et al., 2002; Tie et al., 2007). However, HCHO measured at Tijuana was comparable to or only slightly lower than those in many U.S. urban areas (Dasgupta et al., 2005). The  $P_{\text{OH},\text{HCHO}}/P_{\text{OH},\text{O}_3}$  ratio may serve as a better indicator to assess the contribution of HCHO to the photochemical reactivity among different environment, since photolysis of  $\text{O}_3$  is the most important and ubiquitous OH source in the troposphere and both HCHO and  $\text{O}_3$  are photolyzed by solar radiation within a similar wavelength range and hence the uncertainty associated with the cloudless assumption in the actinic flux calculation can be canceled out. Several HCHO observations in different environments and the calculated  $P_{\text{OH},\text{HCHO}}/P_{\text{OH},\text{O}_3}$  ratios are tabulated in Table 1 for inter-comparison. The lowest HCHO concentration of 1.5 ppbv is measured at a rural site in China and its

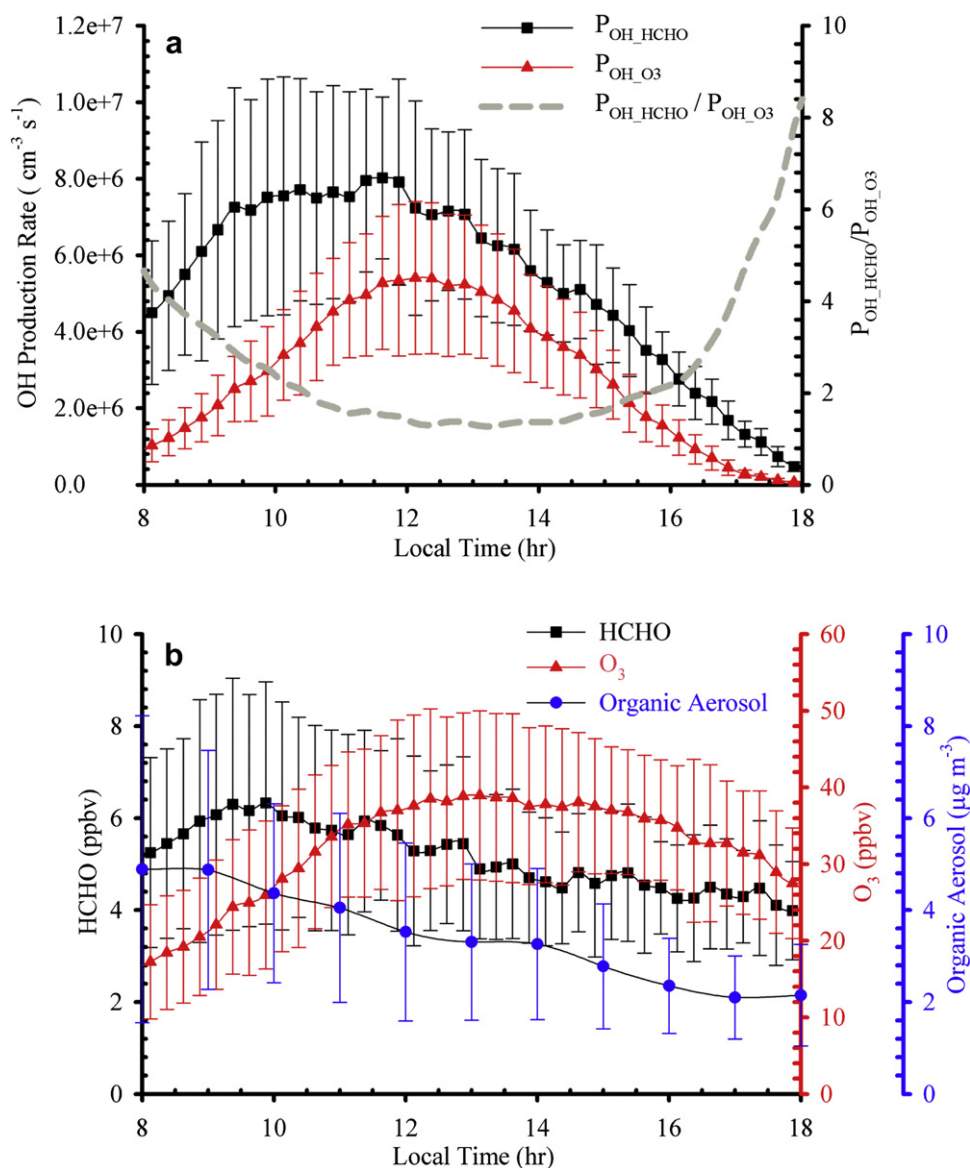


**Fig. 5.** a) Daytime OH radical production rates calculated from photolysis of HCHO and  $\text{O}_3$  and the ratio of the two; b) The corresponding HCHO,  $\text{O}_3$ , and organic aerosol concentrations. All error bars represent  $\pm\sigma$ .

**Table 1**

Inter-comparisons of HCHO observations and the  $P_{\text{OH\_HCHO}}/P_{\text{OH\_O}_3}$  ratios among various environments.

Site location	Site type	Mean HCHO (PPBV)	Mean $P_{\text{OH\_HCHO}}/P_{\text{OH\_O}_3}$	Reference
Tijuana, Mexico	Urban	4.0	4.66	This work
Mazhuang, Shandong, China	Rural	1.5	0.13	(Wang et al., 2010b)
Mexico City, Mexico	Urban	8.2	$\sim 1.0$	(Garcia et al., 2006; Volkamer et al., 2010)
Rome, Italy	Urban	18 (summer) 10 (winter)	10–100	(Werner et al., 1999)
Various U.S. Metropolitan Areas	Urban	3.1–8.0	N/A	(Dasgupta et al., 2005)

contribution to OH production is estimated to be only  $\sim 13\%$  of that of  $\text{O}_3$ . Among all the urban area observations, Tijuana shows a moderate level of mean HCHO and relatively low  $P_{\text{OH\_HCHO}}/P_{\text{OH\_O}_3}$  ratio. The magnitude of air pollution level in Mexico City is significantly higher than that in Tijuana, with substantially higher  $\text{NO}_x$  and VOC emissions (Fortner et al., 2009; Molina et al., 2002, 2007; Zheng et al., 2008), complicating the interpretation of the role of HCHO. Although the magnitude of  $P_{\text{OH\_HCHO}}$  in Mexico City is on the order of  $1 \times 10^7 \text{ cm}^3 \text{s}^{-1}$ , much higher than that in Tijuana,  $P_{\text{OH\_HCHO}}/P_{\text{OH\_O}_3}$  in Mexico City is around 1.0, indicating a moderate contribution of HCHO to OH production. The considerably higher value of  $P_{\text{OH\_HCHO}}/P_{\text{OH\_O}_3}$  observed in Rome, Italy is probably due to intense traffic near the sampling location, indicating the strong influence from primary HCHO emission. Overall, it is clearly shown that anthropogenic activities in urban environments contribute significant to primary HCHO emission and thus play an important role in regulating the OH radical budget. This is especially the case in Tijuana, where  $\text{O}_3$  concentration is much lower than most North America urban areas.



#### 4. Summary and conclusions

Ambient formaldehyde along with other volatile organic compounds has been measured using a proton-transfer reaction mass spectrometer at a ground site along the U.S.–Mexico border during the Cal-Mex 2010 air quality study. During the observation period, HCHO mixing ratio varies between 1.0 ppbv and 13.7 ppbv. On average, a daily maximum of  $6.3 \pm 2.6$  ppbv is observed around 10 AM and the minimum of  $2.8 \pm 1.3$  occurs around midnight. The daily maximum is reached approximately 3-h before the solar noon, indicating the presence of primary HCHO sources and a fast photolysis loss of HCHO in the early afternoon. The low measured values in the ratio of HCHO to acetaldehyde ( $2.5 \pm 0.8$ ) is consistent with the fact that the observation site is located at an arid area with little vegetation coverage and a strong acetaldehyde emission is expected due to ethanol containing gasoline usage. Using a FTUV model, we simulate the photolysis rates of  $O_3$  and HCHO during the study period and evaluate the relative strength of OH radical production from HCHO photolysis relative to  $O_3$  photolysis.  $POH_{HCHO}/POH_{O_3}$  varies from 0.8 to 18, with the highest values observed around traffic rush hours and may serve as a better indicator of the contribution of HCHO to the local photochemistry. For example, Tijuana has a much lower level of HCHO than Mexico City, but a much higher  $POH_{HCHO}/POH_{O_3}$  ratio, indicating that HCHO in Tijuana plays a more important role than  $O_3$  in contributing to OH radicals and the photochemistry. Diesel vehicles emit higher levels of formaldehyde than do gasoline vehicles.

Our findings suggest that anthropogenic activities, especially the transportation sector, in the Tijuana area contribute significant to primary HCHO emission, especially in the early morning rush hours. Freshly emitted HCHO contributes to OH production that leads to further HCHO photochemical formation with a higher magnitude than primary emissions. Also, since diesel vehicles emit higher levels of formaldehyde than do gasoline vehicles, the relative importance of diesel fuel use, compared to gasoline use, may also contribute to the significant primary HCHO emission in this study area.

Our results indicate that the primary HCHO emission in Tijuana plays a dominant role in regulating OH radical budget and thus degradation of other primary air pollutants and formation of secondary pollutants, including ozone and secondary organic aerosols. An effective control measure of the mobile sources can potentially reduce the photochemical reactivity in this region, which shall be further investigated using more robust atmospheric chemical model simulations.

#### Acknowledgments

This work was supported by the National Science Foundation (AGS-1009727 and AGS-1009393), the Robert Welch Foundation (SA-1417), the California Air Resources Board (09-356), and the Mexican National Institute of Ecology. We acknowledged Alejandro Torres-Jaramillo and Jose Santos Garcia-Yee for their support with the CCA-UNAM air quality mobile monitoring station during the campaign. J.Z. and Y.M. acknowledged support from the National Natural Science Foundation of China (40905057) and Jiangsu University Natural Science Research Foundation (09KJB170004). G. Li acknowledged support from MIT Molina Fellowship.

#### References

- Aiken, A.C., Salcedo, D., Cubison, M.J., Huffman, J.A., DeCarlo, P.F., Ulbrich, I.M., Docherty, K.S., Sueper, D., Kimmel, J.R., Worsnop, D.R., Trimborn, A., Northway, M., Stone, E.A., Schauer, J.J., Volkamer, R., Fortner, E., de Foy, B., Wang, J., Laskin, A., Shutthanandan, V., Zheng, J., Zhang, R., Gaffney, J., Marley, N.A., Paredes-Miranda, G., Arnott, W.P., Molina, L.T., Sosa, G.,

- Jimenez, J.L., 2009. Mexico City aerosol analysis during MILAGRO using high resolution aerosol mass spectrometry at the urban supersite (T0) – part 1: fine particle composition and organic source apportionment. *Atmos. Chem. Phys.* 9, 6633–6653.
- Aiken, A.C., de Foy, B., Wiedinmyer, C., DeCarlo, P.F., Ulbrich, I.M., Wehrli, M.N., Szidat, S., Prevot, A.S.H., Noda, J., Wacker, L., Volkamer, R., Fortner, E., Wang, J., Laskin, A., Shutthanandan, V., Zheng, J., Zhang, R., Paredes-Miranda, G., Arnott, W.P., Molina, L.T., Sosa, G., Querol, X., Jimenez, J.L., 2010. Mexico City aerosol analysis during MILAGRO using high resolution aerosol mass spectrometry at the urban supersite (T0) – part 2: analysis of the biomass burning contribution and the modern carbon fraction. *Atmos. Chem. Phys.* 10, 5315–5341.
- Alzueta, M.U., Glarborg, P., 2003. Formation and destruction of  $CH_2O$  in the exhaust system of a gas engine. *Environ. Sci. Technol.* 37, 4512–4516.
- Ammann, C., Brunner, A., Spirig, C., Neftel, A., 2006. Technical note: water vapour concentration and flux measurements with PTR-MS. *Atmos. Chem. Phys.* 6, 4643–4651.
- Anderson, L.G., Lanning, J.A., Barrell, R., Miyagishima, J., Jones, R.H., Wolfe, P., 1996. Sources and sinks of formaldehyde and acetaldehyde: an analysis of Denver's ambient concentration data. *Atmos. Environ.* 30, 2113–2123.
- Anderson, L.G., 2009. Ethanol fuel use in Brazil: air quality impacts. *Energy Environ. Sci.* 2, 1015–1037.
- Atkinson, R., Arey, J., 2003. Atmospheric degradation of volatile organic compounds. *Chem. Rev.* 103, 4605–4638.
- Blanchard, C.L., 1999. Methods for attributing ambient air pollutants to emission sources. *Annu. Rev. Energy Env.* 24, 329–365.
- Bravo, H.A., Torres, R.J., 2000. The usefulness of air quality monitoring and air quality impact studies before the introduction of reformulated gasolines in developing countries Mexico City, a real study case. *Atmos. Environ.* 34, 499–506.
- Buzcu Guven, B., Olague, E.P., 2011. Ambient formaldehyde source attribution in Houston during TexAQS II and TRAMP. *Atmos. Environ.* 45, 4272–4280.
- Carlier, P., Hannachi, H., Mouvrier, G., 1986. The chemistry of carbonyl-compounds in the atmosphere – a review. *Atmos. Environ.* 20, 2079–2099.
- Dasgupta, P.K., Li, J.Z., Zhang, G.F., Luke, W.T., McClenny, W.A., Stutz, J., Fried, A., 2005. Summertime ambient formaldehyde in five US metropolitan areas: Nashville, Atlanta, Houston, Philadelphia, and Tampa. *Environ. Sci. Technol.* 39, 4767–4783.
- Fan, J.W., Zhang, R.Y., 2004. Atmospheric oxidation mechanism of isoprene. *Environ. Chem.* 1, 140–149.
- Fan, J.W., Zhang, R.Y., Collins, D., Li, G.H., 2006. Contribution of secondary condensable organics to new particle formation: a case study in Houston, Texas. *Geophys. Res. Lett.* 33, L15802.
- Finlayson-Pitts, B.J., Pitts, J.N., 1999. *Chemistry of the Upper and Lower Atmosphere: Theory, Experiments and Applications*. Academic Press, San Diego, Calif.
- Fortner, E.C., Zheng, J., Zhang, R., Knighton, B.W., Volkamer, R.M., Sheehy, P., Molina, L., André, M., 2009. Measurements of volatile organic compounds using proton transfer reaction – mass spectrometry during the MILAGRO 2006 campaign. *Atmos. Chem. Phys.* 9, 467–481.
- Friedfeld, S., Fraser, M., Ensor, K., Tribble, S., Rehle, D., Leleux, D., Tittel, F., 2002. Statistical analysis of primary and secondary atmospheric formaldehyde. *Atmos. Environ.* 36, 4767–4775.
- Garcia, A.R., Volkamer, R., Molina, L.T., Molina, M.J., Samuelson, J., Mellqvist, J., Galle, B., Herndon, S.C., Kolb, C.E., 2006. Separation of emitted and photochemical formaldehyde in Mexico City using a statistical analysis and a new pair of gas-phase tracers. *Atmos. Chem. Phys.* 6, 4545–4557.
- Gratien, A., Nilsson, E., Doussin, J.F., Johnson, M.S., Nielsen, C.J., Stenstrom, Y., Picquet-Varrault, B., 2007. UV and IR absorption cross-sections of HCHO, HCDO, and DCDO. *J. Phys. Chem. A* 111, 11506–11513.
- Hansel, A., Jordan, A., Holzinger, R., Prazeller, P., Vogel, W., Lindinger, W., 1995. Proton-transfer reaction mass-spectrometry - online trace gas-analysis at the ppb level. *Int. J. Mass. Spectrom.* 149, 609–619.
- Hansel, A., Singer, W., Wisthaler, A., Schwarzmann, M., Lindinger, W., 1997. Energy dependencies of the proton transfer reactions  $H_3O^+ + CH_2O \rightleftharpoons CH_2OH^+ + H_2O^+$ . *Int. J. Mass. Spectrom.* 167, 697–703.
- Hodzic, A., Jimenez, J.L., 2011. Modeling anthropogenically controlled secondary organic aerosols in a megacity: a simplified framework for global and climate models. *Geosci. Model. Dev.* 4, 901–917.
- Karl, T., Jobson, T., Kuster, W.C., Williams, E., Stutz, J., Shetter, R., Hall, S.R., Goldan, P., Fehsenfeld, F., Lindinger, W., 2003. Use of proton-transfer-reaction mass spectrometry to characterize volatile organic compound sources at the La Porte super site during the Texas Air Quality Study 2000. *J. Geophys. Res.* 108, 4508.
- Khalizov, A.F., Xue, H., Zhang, R., 2009. Enhanced light absorption and scattering by carbon soot aerosols internally mixed with sulfuric acid. *J. Phys. Chem.* 113, 1066–1074.
- Lee, Y.N., Zhou, X., Kleinman, L.L., Nunnermacker, L.J., Springston, S.R., Daum, P.H., Newman, L., Keigley, W.G., Holdren, M.W., Spicer, C.W., Young, V., Fu, B., Parrish, D.D., Holloway, J., Williams, J., Roberts, J.M., Ryerson, T.B., Fehsenfeld, F.C., 1998. Atmospheric chemistry and distribution of formaldehyde and several multioxygenated carbonyl compounds during the 1995 Nashville Middle Tennessee Ozone Study. *J. Geophys. Res.* 103, 22449–22462.
- Lei, W., Zhang, R., McGivern, W.S., Derocskai-Kovacs, A., North, S.W., 2000a. Theoretical study of isomeric branching in the isoprene-OH reaction: implications to final product yields in isoprene oxidation. *Chem. Phys. Lett.* 326, 109–114.
- Lei, W., Derocskai-Kovacs, A., Zhang, R., 2000b. Ab initio study of OH addition reaction to isoprene. *J. Chem. Phys.* 113, 5354–5360.

- Lei, W., Zhang, R., 2001. Theoretical study of hydroxy-isoprene alkoxy radicals and their decomposition pathways. *J. Phys. Chem.* 105, 3808–3815.
- Lei, W., Zavala, M., de Foy, B., Volkamer, R., Molina, M.J., Molina, L.T., 2009. Impact of primary formaldehyde on air pollution in the Mexico City Metropolitan Area. *Atmos. Chem. Phys.* 9, 2607–2618.
- Lei, W.F., Zhang, R.Y., Tie, X.X., Hess, P., 2004. Chemical characterization of ozone formation in the Houston-Galveston area: a chemical transport model study. *J. Geophys. Res.* 109, D12301.
- Li, G.H., Zhang, R.Y., Fan, J.W., Tie, X.X., 2005. Impacts of black carbon aerosol on photolysis and ozone. *J. Geophys. Res.* 110, D23206. <http://dx.doi.org/10.1029/2005JD005898>.
- Li, G.H., Zhang, R.Y., Fan, J.W., Tie, X.X., 2007. Impacts of biogenic emissions on photochemical ozone production in Houston, Texas. *J. Geophys. Res.* 112, D10309. <http://dx.doi.org/10.1029/2006JD007924>.
- Li, J.Z., Dasgupta, P.K., Luke, W., 2005. Measurement of gaseous and aqueous trace formaldehyde – revisiting the pentanediol reaction and field applications. *Anal. Chim. Acta* 531, 51–68.
- Lindinger, W., Hansel, A., Jordan, A., 1998. On-line monitoring of volatile organic compounds at pptv levels by means of proton-transfer-reaction mass spectrometry (PTR-MS) – medical applications, food control and environmental research. *Int. J. Mass. Spectrom.* 173, 191–241.
- Mitchell, C.E., Olsen, D.B., 2000. Formaldehyde formation in large bore natural gas engines part 1: formation mechanisms. *J. Eng. Gas. Turbines Power-trans. ASME* 122, 603–610.
- Molina, L.T., Molina, M.J., Alliance for Global Sustainability, 2002. *Air Quality in the Mexico Megacity: An Integrated Assessment*. Kluwer Academic Publishers, Dordrecht, Boston.
- Molina, L.T., Kolb, C.E., de Foy, B., Lamb, B.K., Brune, W.H., Jimenez, J.L., Ramos-Villegas, R., Sarmiento, J., Paramo-Figueroa, V.H., Cardenas, B., Gutierrez-Avedoy, V., Molina, M.J., 2007. Air quality in North America's most populous city – overview of the MCMA-2003 campaign. *Atmos. Chem. Phys.* 7, 2447–2473.
- Okuyama, K., Kousaka, Y., Motouchi, T., 1984. Condensational growth of ultrafine aerosol-particles in a new particle-size magnifier. *Aerosol. Sci. Technol.* 3, 353–366.
- Parrish, D.D., Ryerson, T.B., Mellqvist, J., Johansson, J., Fried, A., Richter, D., Walega, J.G., Washenfelder, R.A., de Gouw, J.A., Peischl, J., Aikin, K.C., McKeen, S.A., Frost, G.J., Fehsenfeld, F.C., Herndon, S.C., 2012. Primary and secondary sources of formaldehyde in urban atmospheres: Houston Texas region. *Atmos. Chem. Phys.* 12, 3273–3288.
- Rappengluck, B., Dasgupta, P.K., Leuchner, M., Li, Q., Luke, W., 2010. Formaldehyde and its relation to CO, PAN, and SO<sub>2</sub> in the Houston-Galveston airshed. *Atmos. Chem. Phys.* 10, 2413–2424. <http://dx.doi.org/10.5194/acp-10-2413-2010>.
- Sakugawa, H., Kaplan, I.R., 1993. Comparison of H<sub>2</sub>O<sub>2</sub> and O<sub>3</sub> content in atmospheric samples in the San-Bernardino Mountains, Southern California. *Atmos. Environ.* 27, 1509–1515.
- Shepson, P.B., Hastie, D.R., Schiff, H.I., Polizzi, M., Bottenheim, J.W., Anlauf, K., Mackay, G.I., Karecki, D.R., 1991. Atmospheric concentrations and temporal variations of C<sub>1</sub>–C<sub>3</sub> carbonyl-compounds at 2 rural sites in central Ontario. *Atmos. Environ.* 25, 2001–2015.
- Steinbacher, M., Dommen, J., Ammann, C., Spirig, C., Neftel, A., Prevot, A.S.H., 2004. Performance characteristics of a proton-transfer-reaction mass spectrometer (PTR-MS) derived from laboratory and field measurements. *Int. J. Mass. Spectrom.* 239, 117–128.
- Takahama, S., Johnson, A., Morales, J.G., Russell, L.M., Duran, R., Rodriguez, G., Zheng, J., Zhang, R., Toom-Saunty, D., Leaitch, W.R., 2012. Submicron organic aerosol in Tijuana, Mexico, from local and Southern California sources during the CalMex campaign. *Atmos. Environ.* 62. <http://dx.doi.org/10.1016/j.atmosenv.2012.07.057>.
- Tanner, R.L., Miguel, A.H., Deandrade, J.B., Gaffney, J.S., Streit, G.E., 1988. Atmospheric chemistry of aldehydes – enhanced peroxyacetyl nitrate formation from ethanol-fueled vehicular emissions. *Environ. Sci. Technol.* 22, 1026–1034.
- Tie, X.X., Madronich, S., Walters, S., Zhang, R.Y., Rasch, P., Collins, W., 2003. Effect of clouds on photolysis and oxidants in the troposphere. *J. Geophys. Res.* 108, 4642. <http://dx.doi.org/10.1029/2003JD003659>.
- Tie, X.X., Madronich, S., Walters, S., Edwards, D.P., Ginoux, P., Mahowald, N., Zhang, R.Y., Lou, C., Brasseur, G., 2005. Assessment of the global impact of aerosols on tropospheric oxidants. *J. Geophys. Res.* 110, D03204.
- Tie, X., Madronich, S., Li, G., Ying, Z., Zhang, R., Garcia, A., Lee-Taylor, J., Liu, Y., 2007. Characterizations of chemical oxidants in Mexico City: a regional chemical dynamical model (WRF-Chem) study. *Atmos. Environ.* 41, 1989–2008.
- Volkamer, R., Sheehy, P., Molina, L.T., Molina, M.J., 2010. Oxidative capacity of the Mexico City atmosphere – part 1: a radical source perspective. *Atmos. Chem. Phys.* 10, 6969–6991.
- Wagner, T., Wyszynski, M.L., 1996. Aldehydes and ketones in engine exhaust emissions – a review. *Proc. Inst. Mech. Engineers Part D – J. Automobile Eng.* 210, 109–122.
- Wang, L., Lal, V., Khalizov, A.F., Zhang, R., 2010a. Heterogeneous chemistry of alkylamines with sulfuric acid: implications for atmospheric formation of alkylammonium sulfates. *Environ. Sci. Technol.* 44, 2461–2465. <http://dx.doi.org/10.1021/es9036868>.
- Wang, X.Y., Wang, H.X., Wang, S.L., 2010b. Ambient formaldehyde and its contributing factor to ozone and OH radical in a rural area. *Atmos. Environ.* 44, 2074–2078.
- Werner, G., Kastler, J., Looser, R., Ballschmiter, K., 1999. Organic nitrates of isoprene as atmospheric trace compounds. *Angew. Chem. Int. Edit.* 38, 1634–1637.
- Zhang, R., Suh, I., Lei, W., Clinkenbeard, A.D., North, S.W., 2000. Kinetic studies of OH-initiated reactions of isoprene. *J. Geophys. Res.* 105, 24627–24635.
- Zhang, D., Lei, W.F., Zhang, R.Y., 2002. Mechanism of OH formation from ozonolysis of isoprene: kinetics and product yields. *Chem. Phys. Lett.* 358, 171–179.
- Zhang, R., Tie, X., Bond, D.W., 2003. Impacts of anthropogenic and natural NO<sub>x</sub> sources over the U.S. on tropospheric chemistry. *Proc. Natl. Acad. Sci. U S A* 100, 1505–1509.
- Zhang, R., Lei, W.F., Tie, X.X., Hess, P., 2004. Industrial emissions cause extreme urban ozone diurnal variability. *Proc. Natl. Acad. Sci. U S A* 101, 6346–6350.
- Zhang, R., Khalizov, A.F., Pagels, J., Zhang, D., Xue, H., McMurry, P.H., 2008. Variability in morphology, hygroscopic and optical properties of soot aerosols during internal mixing in the atmosphere. *Proc. Natl. Acad. Sci. U S A* 105, 10291–10296.
- Zhang, R., Wang, L., Khalizov, A.F., Zhao, J., Zheng, J., McGraw, R.L., Molina, L.T., 2009. Formation of nanoparticles of blue haze enhanced by anthropogenic pollution. *Proc. Natl. Acad. Sci. U S A* 106, 17650–17654.
- Zhang, R., Khalizov, A.F., Wang, L., Hu, M., Wen, X., 2012. Nucleation and growth of nanoparticles in the atmosphere. *Chem. Rev.* 112, 1957–2011.
- Zhao, J., Zhang, R., 2004. Proton transfer reaction rate constants between hydronium ion (H<sub>3</sub>O<sup>+</sup>) and volatile organic compounds. *Atmos. Environ.* 38, 2177–2185.
- Zhao, J., Zhang, R., Fortner, E.C., North, S.W., 2004. Quantification of hydroxycarbonyls from OH-isoprene reactions. *J. Am. Chem. Soc.* 126, 2686–2687.
- Zhao, J., Zhang, R.Y., Misawa, K., Shibuya, K., 2005a. Experimental product study of the OH-initiated oxidation of m-xylene. *J. Photoch. Photobio. A* 176, 199–207.
- Zhao, J., Levitt, N.P., Zhang, R., 2005b. Heterogeneous chemistry of octanal and 2,4-hexadienal with sulfuric acid. *Geophys. Res. Lett.* 32, L09802. <http://dx.doi.org/10.1029/2004GL022200>.
- Zhao, J., Levitt, N.P., Zhang, R.Y., Chen, J.M., 2006. Heterogeneous reactions of methylglyoxal in acidic media: implications for secondary organic aerosol formation. *Environ. Sci. Technol.* 40, 7682–7687.
- Zhao, J., Khalizov, A., Zhang, R.Y., McGraw, R., 2009. Hydrogen-bonding interaction in molecular complexes and clusters of aerosol nucleation precursors. *J. Phys. Chem. A* 113, 680–689.
- Zheng, J., Zhang, R., Fortner, E.C., Volkamer, R.M., Molina, L., Aiken, A.C., Jimenez, J.L., Gaeggeler, K., Dommen, J., Dusanter, S., Stevens, P.S., Tie, X., 2008. Measurements of HNO<sub>3</sub> and N<sub>2</sub>O<sub>5</sub> using ion drift-chemical ionization mass spectrometry during the MILAGRO/MCMA-2006 campaign. *Atmos. Chem. Phys.* 8, 6823–6838.
- Zheng, J., Khalizov, A., Wang, L., Zhang, R., 2010. Atmospheric pressure-ion drift chemical ionization mass spectrometry for detection of trace gas species. *Anal. Chem.* 82, 7302–7308.